CHAPTER 3

ZnO Tetrapods Network Applied as UV Sensor

Surrounded by a number of the ZnO nanostructures morphologies, the tetrapod-like ZnO (T-ZnO) was the one of the motivating structures since it exhibits three dimension of the geometry with there are four rod-shaped legs that connected together at the main of axis center with the tetrahedral angles type[36]. This ZnO morphology was appropriate for a number of semiconducting of electronic devices. The UV sensors, the one of the possible appliance for environmentally friendly and soldierly sensing, based on T-ZnO were can arrange for high UV light sensitivity with time properties such as rapidly response time and recovery time. This was for the reason that the tetrapod-like ZnO had the great surface-to-volume ratio and advanced light sparseness on the ZnO surface [36].

In view of the operation procedures, the ultraviolet-generated the charge carries were desired to obtain the electrodes moving through of the physically-touching legs of tetrapod-like ZnO network. The tetrapod-like ZnO which has the charge transfer through the grain boundaries was generally restrictive by the potential barrier shaped next to the boundary of nano-junction among tetrapod-like ZnO's legs [36]. So that be successful a higher UV light responsibility, this potential barrier ought to been reduced.

In this chapter work, we have presented a UV sensor based on ZnO tetrapod network or ITN-ZnO, which was easily and rapidly synthesized by microwave-assisted thermal oxidation (MWTO)[70]. The ITN-ZnO was tetrapod-like of the geometry with leg-to-leg linked jointly via the coulombic interaction. The ultraviolet light sensors that were built from the ITN-ZnO has exposed the superior electrical property in analogy with that created from ZnO powder (P-ZnO) and ZnO tetrapod (T-ZnO) and built the UV light sensor based on the ITN-ZnO and characterized it via impedance spectroscopy

to take forward understanding into the charge transfer mechanisms of the ITN-ZnO sensor. The obtained results display impressive charge transfer actions with lower the potential barrier at the grain boundary in analogy with the UV light sensor devices of the P-ZnO and T-ZnO. The UV light sensing properties of sensor devices had also been reported.

3.1 Fabrication of UV sensor

Sensors devices constructed from different morphologies of ZnO (ITN-ZnO, T-ZnO and ZnO powder (P-ZnO; Sigma-Aldrich, average size b 1μm, purity 99.9%)) were fabricated and compared. Gold interdigital electrodes coated alumina plates were used as substrates for the sensors in **Fig.3.1.** Mixtures of various ZnO structure materials (ITN-ZnO, T-ZnO and ZnO powder) with ethanol were screen-printed on the alumina substrates. Measurement of UV sensing properties was performed by biasing the sensors with DC voltage at 1V and detecting output DC current and resistance. The measurement was operated under UVA (λ = 365 nm) irradiation from light source with different intensity of 1, 2, 3, 4 and 5 mW/cm^2 at room temperature. A schematic illustration of the measurement is shown in **Fig.3.2** Impedance spectroscopy was performed to investigate charge dynamics of the devices by using sinusoidal potential amplitude of 20 mV in a frequency range from 1 Hz to 10,000 Hz under UV irradiation.

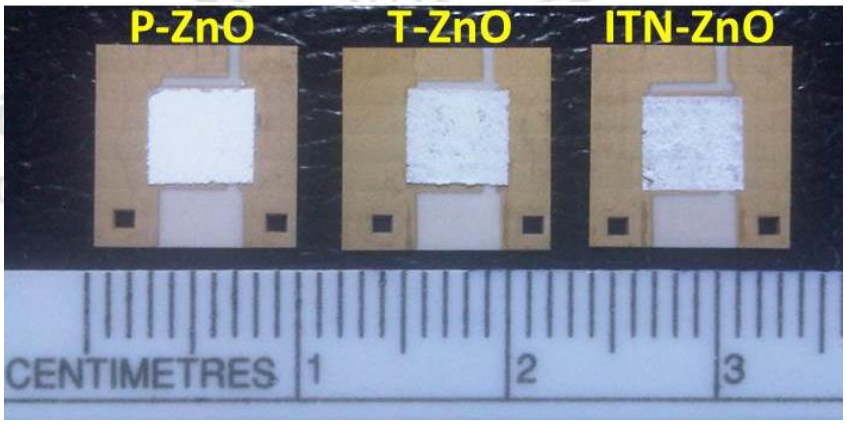

Figure 3.1 Optical image showing three ZnO samples with area of about 5x5 mm^2 on substrate electrode.

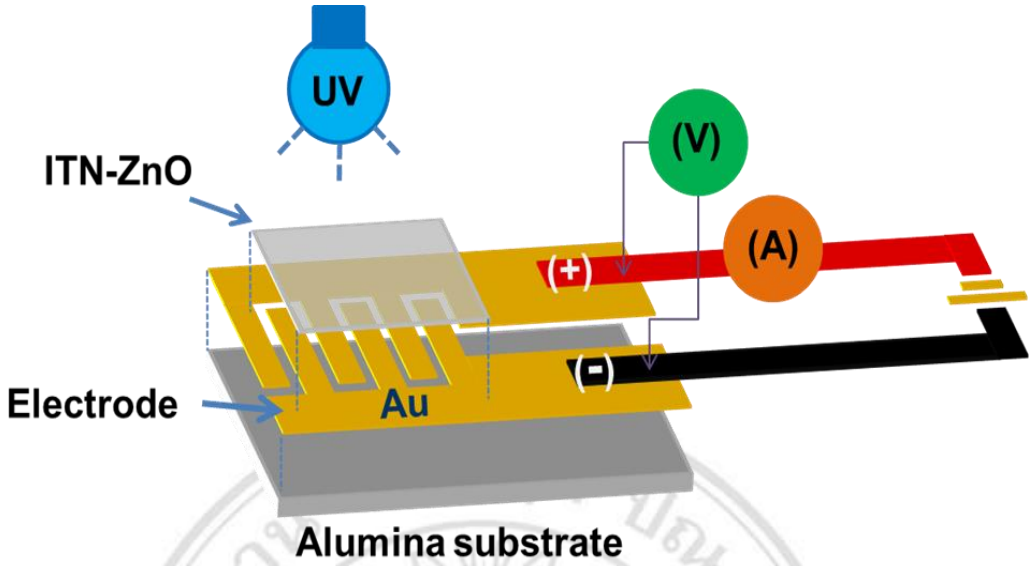

Figure 3.2 The schematic illustration of the measurement used for UV sensing characteristics. For fabrication of ITN-ZnO sensor that under UV light was screened on alumina substrate with gold inter-digital electrodes. Pt wires were connected to electrodes and put in UV box with UV lamps. Reprinted with permission from ref [86]. Copyright (2016) Elsevier.

3.2 Optical properties of ITN-ZnO

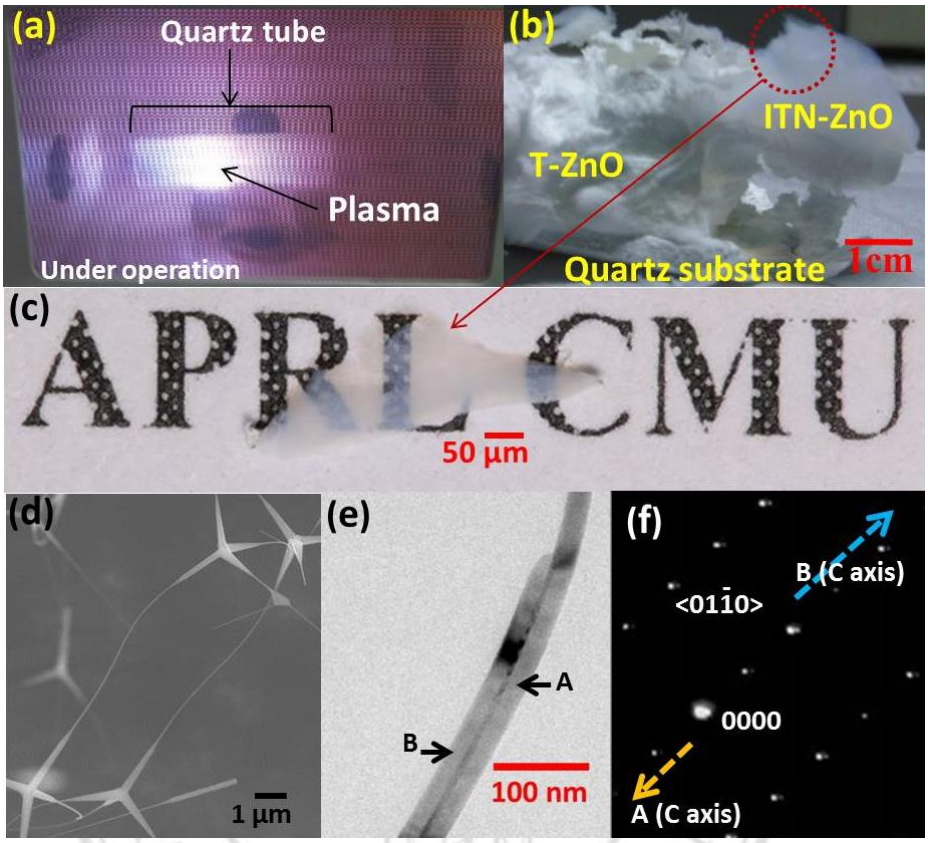

Figure 3.3 The optical image of ITN-ZnO nanostructures that (a) the specimens were irradiated by the microwave oven for household of and (b) the products had obtained already after MWTO, (c) ITN-ZnO was shown translucent properties upper region of it, (d) the FE-SEM that is the field emission scanning electron microscopy image of ITN-ZnO, and (e) the connection between legs of ITN-ZnO was shown by the bright field transmission electron microscopy (TEM) image (f) the selected area diffraction pattern (SADP) technique result of ITN-ZnO. Reprinted with permission from ref [86]. Copyright (2016) Elsevier.

For the result, the camera images of the plasma occurred in a course of the microwave oven arcing technique and the wool-like ZnO produces collected after the electromagnetics wave arcing process was shown in the **Fig. 3.3a and 3.3b**. It shown very clearly that the producers of as-synthesized ZnO, had dual disparate shape of ZnO nanostructures, which refers to dual divergent the morphologies as was reported in our previous work [11]. Coarse white color wool-like ZnO produce in the bottom region was T-ZnO and the upstairs translucent wool-like ZnO produce is the ITN-ZnO where their legs were connected via columbic interaction structure network, shown in the **Fig. 3.3d and 3.3e.** TEM result of the selected area diffraction pattern (SADP) analysis of the TN-ZnO in **Fig. 3.3(f)** had as well confirmed that these legs grow along the direction of c-axis <0001> of TN-ZnO interlinked of legs.

Moreover, the normalized Photoluminescence Spectroscopy (PL spectra) result of all samples (**Fig 3.4**) was shown dual luminescence bands such as (1) a narrow band centered at size 386 nm corresponding to close the band edge the emission of ZnO that the energy gap as 3.22 eV, and (2) the broad band in the visible light region of 440 to 640 nm mentioning to the defects in the crystal of ZnO together with interstitial and the vacancy.

The PL spectra of the specimen display a UV emission band with peak wavelength at 380 nm and a broad visible emission band centered at 530 nm. The UV emission band is attributed to the near band (NB) emission of the ZnO crystal. The broad visible emission band is due to defect level emission that originates from oxygen vacancies in the structures [102].

The PL spectra intensity of the peaks in inter visible light region was relatively lesser than that of the close band edge peaks. Specially, the result of ITN-ZnO displays the lowermost luminescence intensity of the visible light region, indicative of that it had upper sequence of crystallinity between these specimens.

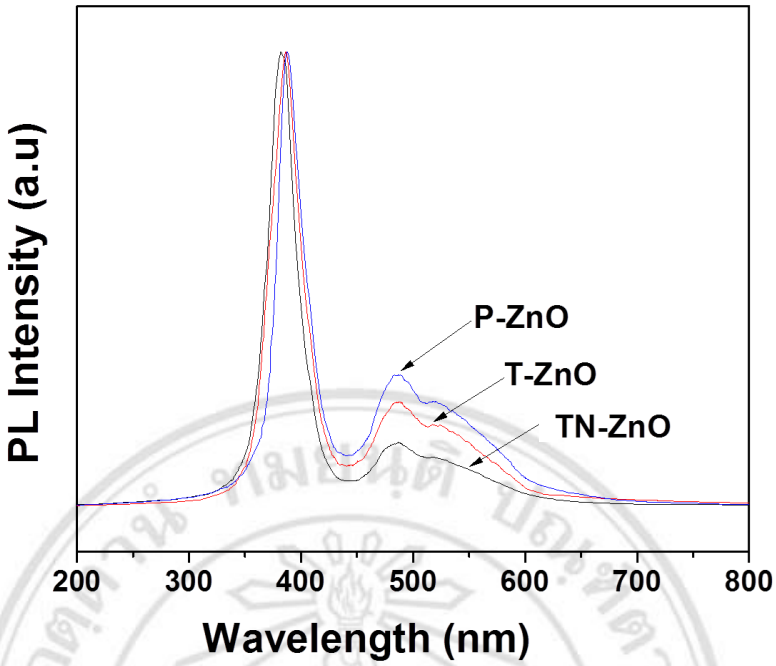

Figure 3.4 The photoluminescence spectrum of ITN-ZnO correlated with P-ZnO and T-ZnO. Reprinted with permission from ref [86]. Copyright (2016) Elsevier.

3.3 Electrical properties of ITN-ZnO under UV light illumination

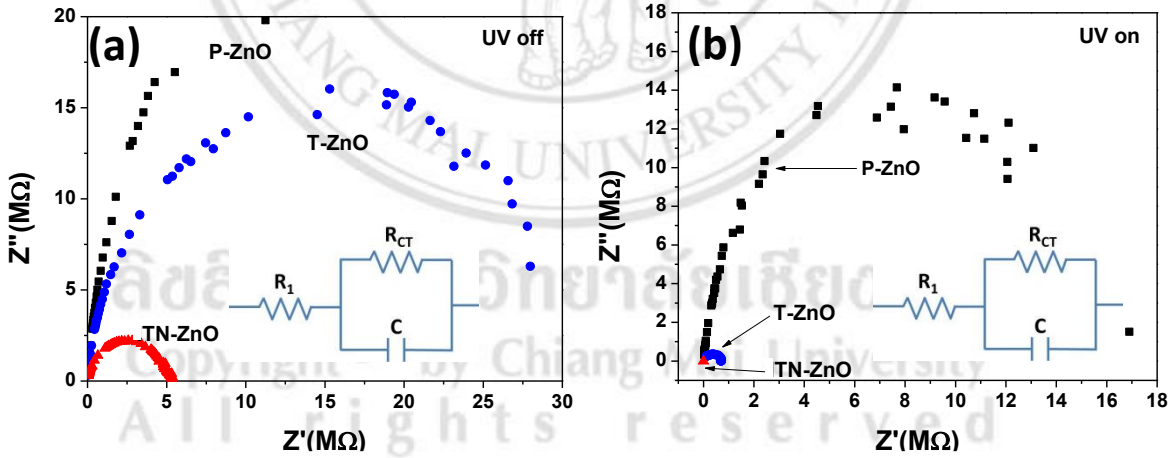

Figure 3.5 The Nyquist plots results of the ultraviolet light sensors were include from T-ZnO, P-ZnO, and ITN-ZnO samples under (a) the UV irradiation and (b) the dark condition. Reprinted with permission from ref [86]. Copyright (2016) Elsevier.

The measurement of the impedance result was hardened characterize the kinetics mechanism of an electron transfer for UV light sensors created from T-ZnO, P-ZnO and ITN-ZnO. The Nyquist plots graph of recorded the impedance spectra were presented

in the **Fig. 3.5**. The experimental data had been fitted via an equivalent circuit of the model as presented in the inset of the **Fig. 3.5** and the result extracted parameters were summarized in the **Table. 3.1**.

Parameters in an equivalent circuit of the model include R_1 refer to the resistance of electrodes, R_{CT} refer to the resistance of ZnO samples of UV sensor and C refer to the capacitance ZnO samples of UV sensor. P-ZnO has highest capacitance because it has highest potential barrier between particles (in **Fig 3.5b**) and it accumulates charges. However, ITN-ZnO has less potential barrier between interlinked ZnO tetrapod networks. This causes electrons to travel through with less capacitance and less resistance (R_{CT}) (in **Table 3.1**).

Table 3.1 the ultraviolet sensor electrical properties of with various ZnO kinds of structure morphology. Reprinted with permission from ref[86]. Copyright (2016) Elsevier.

Type of ZnO structure	**R_1(kΩ) UV on (off)**	**R_{CT}(kΩ) UV on (off)**	**C (pf) UV on (off)**
P-ZnO	21(29)	18000(56000)	60(84)
T-ZnO	16(34)	600(30000)	58(72)
ITN-ZnO	2.8(54)	3(4900)	21(61)

Usually, the impedance spectra of UV light sensors represent three semicircles at low medium, and high frequency regions. But, in this work, the single one of semicircle at medium frequency had been monitored. As shown in the **Fig. 3.3**, the diameters of the arcs were without doubt different. The biggest one was got from the P-ZnO sample of UV sensor. In view of the extracted parameters, the R_1 that refer to the resistance in the equivalent circuit was related to the charge transport resistance of the ZnO materials. The R_{CT} that refer to the charge of transfer resistance and space-charge layer *C* that was capacitance talk about to the charge of transfer at between the ZnO and ZnO boundary and between the ZnO and Au interface. It was shown in the **Table 3.1** that the R_1 of altogether specimen were comparable however then the R_{CT} of ITN-ZnO was significantly lesser than that of the P-ZnO and T-ZnO sensor devices, respectively.

Particularly, the specimens were within ultraviolet radiation, the R_{CT} reduces ever since more charge of carriers were generated, expanding conductivity of the materials. The ITN-ZnO sensor that had the lowest R_{CT} and C was probably due to the coulombic connection among legs that interlinked together of ITN-ZnO, which was can decrease the potential barrier at the boundary. In analogy the ITN-ZnO with the event of T-ZnO and P-ZnO devices, the charge transfer of the ITN-ZnO device was more interesting efficient.

For the UV sensor application experimental result, the sensors based on the nanostructured ZnO which as ITN-ZnO and T-ZnO and commercial available zinc oxide powder (P-ZnO) were fabricated by print scene technique which using alumina substrates with gold inter-digital electrodes as shown in **Fig. 3.2.** The electrical properties result of ITN-ZnO under UV light illumination and under dark in either air or nitrogen ambient were investigated and shown as I-V characteristics plotting with a linear scale in the **Fig. 3.6 (a)** and with a semi-logarithmic scale in **Fig. 3.6 (b).**

A semi-logarithmic scale (butterfly plot I-V curve) was plotted for UV sensors. The dark current has different current value of 1000 times less than that of the UV current.

It could be seen that the current of ITN-ZnO sensor demonstrations the highest value (lowest resistance) at circumstances of under UV illumination in nitrogen ambient. Comparing the experimental UV sensor measurement with the value collected under the dark condition, the lower resistance under UV illumination could be illustrated by the increment of photo-generated electrons motivated by the light absorption phenomena of ZnO nanostructures. Moreover, the further decrease in resistance of UV sensor measured under UV illumination in nitrogen ambient could be illustrated by enhance of conduction-band photoelectrons as decreasing of an oxygen adsorption at the ZnO surface.

Thus, UV light and an oxygen atmosphere play a significant role for electrical properties of ITN-ZnO sensor device

The **Fig. 3.6 (c)** was shown the reversible switching curves of electrical current over and done with the devices for external ZnO morphologies tested under UV illumination in air. When the ultraviolet light was switched on and off respective 200 sec at a stable bias a voltage of 5 V, the on and off current ratio of ITN ZnO shows the highest value of about 7400 was compared to about 2.6 and 0.3 for T-ZnO and P-ZnO sensors. This instructs that the ITN-ZnO sensor shows superior UV detecting properties and clearly be different from the T-ZnO and P-ZnO ones. This might be attributed to an improved transport pathway of ITN-ZnO for electrons that required achieve the Au electrodes. Comparison with T-ZnO and P-ZnO, the ITN-ZnO arrange for negligible effects of grain boundaries that restrict electrons transport, ever since the legs are connected with the columbic interaction as discourse above.

With the intention of examine the properties of sensing of the UV light sensors, typical responses were collected within a number of UV light intensity (1 to 5 W/cm^2) and the results were presented in the **Fig. 3.6(d).** It was seen that very sensors exposed upper resistance ratio at superior ultraviolet light intensity. The ultraviolet sensitivity of specimens improved as a function of ultraviolet light intensity, as shown in **Fig. 3.6(d).** The ITN-ZnO sensor had provided external UV sensor properties with in height and fast response of ultraviolet light. This present that ITN-ZnO show higher ultraviolet sensing properties and vary evidently be different from ZnO powder and ZnO tetrapod.

Interestingly, by comparisons this characteristic properties with the greatest results of previously reported literatures as summarized in the **Table 3.2**, the photo-dark current ratio (I_{uv}/I_{dark}) of our ITN-ZnO sensor device shows higher value (7400) in comparison with that of the other sensor device based on nanotetrapod network of ZnO (4500)[39]. These results propose that the ITN-ZnO had exceptional potential for UV sensor device application.

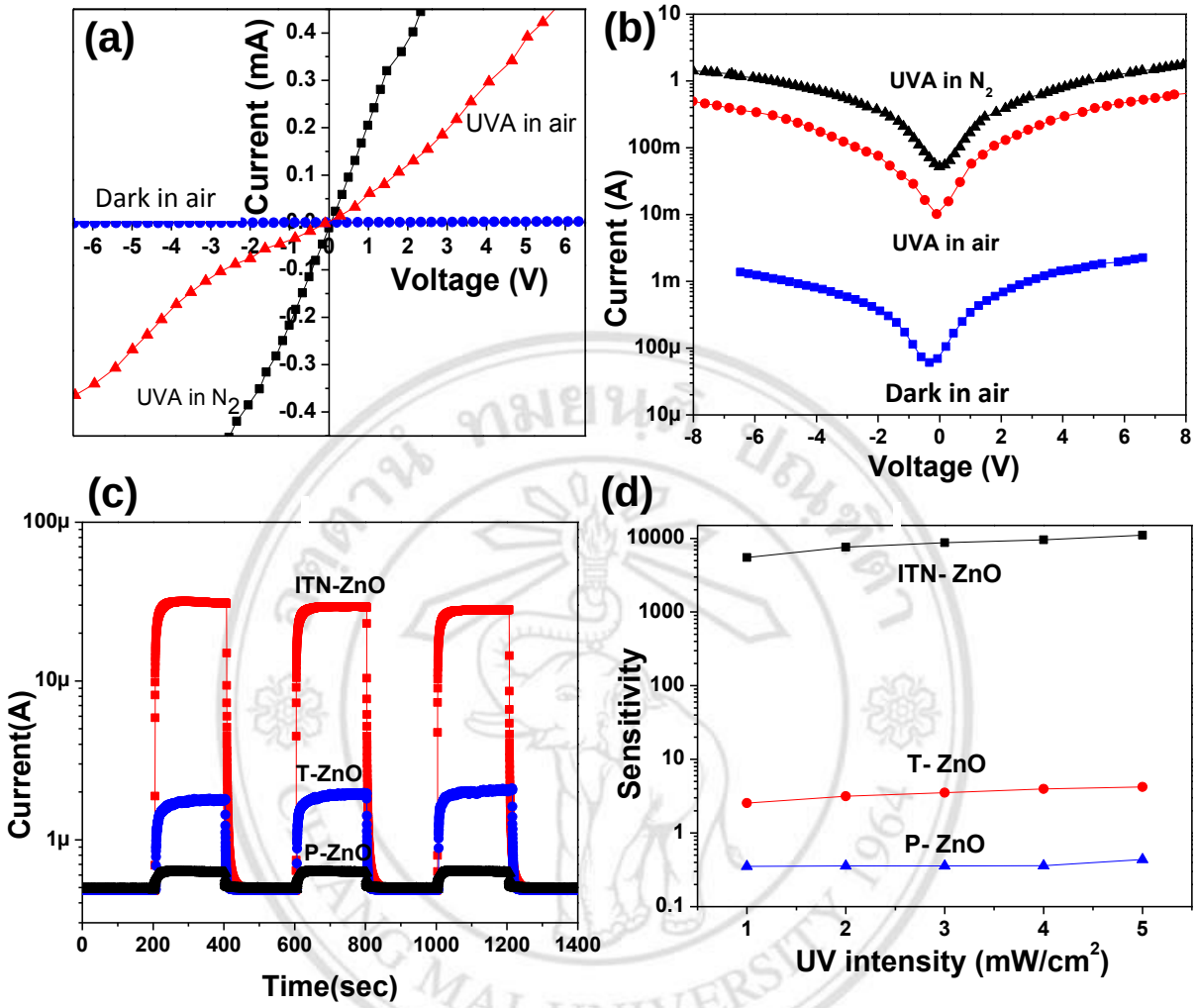

Figure 3.6 The I-V characteristics measurements of ITN-ZnO sensor, monitored within dark and within UV light in either one the air or else nitrogen ambient, plotted the graph (a) in a linear scale and (b) in a semi-logarithmic scale, and (c) reversible switching curves of electrical current for devices conditional different ZnO morphologies. Reprinted with permission from ref [70]. Copyright (2015) American Chemical Society. (d) The photo-dark of resistance ratio that sensitivity was (R_{uv}-R_{dark})/R_{dark})x100 of TN-ZnO, P-ZnO and T-ZnO sensors within UV light by a 365 nm wave length of ultraviolet intensity at a power of 1, 2, 3, 4, and 5 W/cm^2, respectively. Reprinted with permission from ref [86]. Copyright (2016) Elsevier.

Table 3.2. The previously reports of UV sensor/detector based on ZnO nanostructures was concluded by the table list. Reprinted with permission from ref [70]. Copyright (2015) American Chemical Society.

Type of structure	Duration of growth & method	UV intensity 365nm	Bias voltage	I_{UV}/I_{dark}	Rise time	Decay time	Ref
Nanorodnetwork	3-5 h, HT	0.3	4 V	1.8	2 s	-	ref[91
Nano-needle	4 h, CFTS	15-20	0.3 V	312	22 s	7-12 s	ref[39
Nano-tetrapod	<5 s,	15-20	2.4 V	4500	67	30 ms	ref[39
Powder (This work)	Sigma-	2.8	5 V	0.3	4.38	4.76 s	
T-ZnO (This work)	60s,	2.8	5 V	2.6	4.73	2.00 s	
ITN-ZNO(This	60s,	2.8	5 V	7400	3.52	0.67 s	

*MWTO was a microwave-assisted thermal oxidation.

3.4 UV sensing mechanism

To understand, electrical properties and the distinguishable optical of ITN-ZnO sensor from ZnO powder sensor or smooth a freestanding ZnO tetrapod sensor, schematic illustrations shown in the **Fig 3.7(a)** were used to illustrate the current enhance within UV light for the UV light sensing mechanism. The ZnO sensor response variation to within UV illustrations at room temperature could be give details by the energy-band idea of semiconductor, the photoelectric effect, and the superoxide mechanisms.

Ever since zinc oxide had the energy gap (3.3 eV), an electron (e^-) in the valence band (VB) could be excited by ultraviolet type A illustrations from range of 3.10 to 3.94 eV to the conduction band (CB), and leaving a hole (h^+) in the valence band. In this reasons the decrease of the resistance for ZnO tetrapods illuminated with ultraviolet type an illustrations in the air.

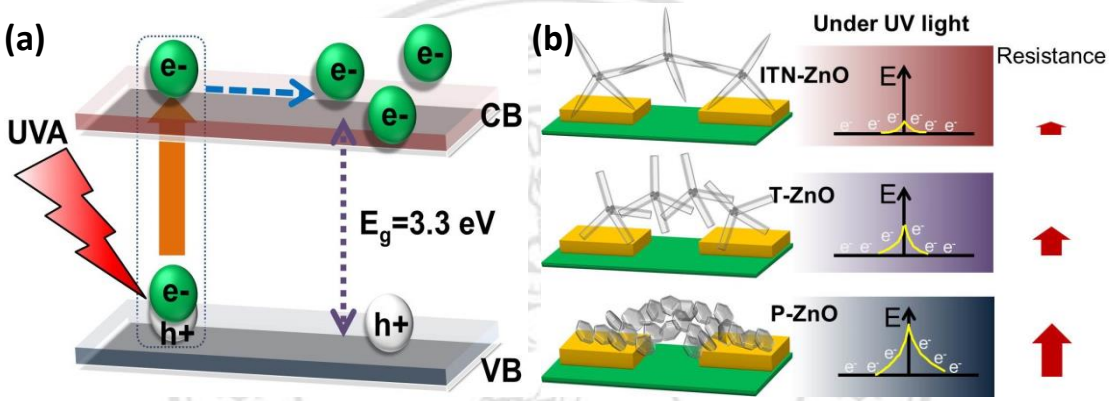

Figure 3.7 (a) The schematic illustration for the ultraviolet light sensing mechanism that able to illustrate the current enhance within ultraviolet light. (b) The conduction or transduction of the mechanism in structure of ZnO: in the P-ZnO, T-ZnO, and ITN-ZnO had the high potential barrier reducing, respectively. Reprinted with permission from ref [86]. Copyright (2016) Elsevier.

On the subject of to the conduction or transduction of the mechanisms in these UV light sensor devices, it was found that the ITN-ZnO sensor had the photo-dark of resistance ratio was significantly superior to that of the P-ZnO and T-ZnO sensor devices. This was motivated by the lessening of the potential barrier at the grain boundary of ITN-ZnO sensor as confirmed by the impedance analysis result. The ultraviolet light generated charge carriers were equipped reach the Au electrode with smaller amount barriers, presentation the dramatic reduce in the sensor resistivity within ultraviolet light in analogy with the extra devices. For that reason, the leg-to-leg linking with coulombic interaction of ITN-ZnO nanostructure significantly decreases the potential barrier at the grain boundary and makes available the efficient of charge transport of the sensor device.

3.5 Chapter Summary

The ZnO nanostructures of UV sensors had been characterized and constructed. The ITN-ZnO sensor device demonstrates the lowermost sensor resistance in analogy with the T-ZnO and P-ZnO ones. The main cause behind schedule the dramatic reduction in sensor resistance was the efficient of charge transfer with small potential barriers at the grain boundary of ZnO. These effects propose that the ITN-ZnO with coulombic leg-to-leg linking was appropriate for efficient ultraviolet light sensor device and another optoelectronic apply devices.